PLANING HULL PERFORMANCE FROM MODEL TESTS

Eric Thornhill*, Dan Oldford**, Neil Bose***, Brian Veitch***, Pengfei Liu*
* Institute for Marine Dynamics, St. John's, Newfoundland, Canada
** Engineering Undergraduate Student, Memorial University, St. John's, Canada
*** Canada Research Chair in Offshore and Underwater Vehicles Design, Faculty of Engineering and Applied Science, Memorial University, St. John's, Newfoundland, Canada

Int. Shipbuild. Progr., **50**, no. 1 & 2 (2003) pp. 5-18

Received: November 2002
Accepted: February 2003

A set of bare hull resistance tests were performed on a 1/8 scale model of an 11.8 m long planing hull. The model was tested over a range of speeds and ballast conditions in calm water. Measurements were made of tow force, running trim, and sinkage. Wetted areas and lengths were determined using underwater video. Flush mounted pressure taps gave gauge pressures at various locations on the hull surface. Wave profiles were measured using an array of capacitance probes positioned laterally in the tank. Boundary layer velocity profiles were resolved at two locations on the hull for several model speeds using a laser Doppler velocimeter (LDV). Pressures under the aft region of the hull were found to be lower and velocities just outside of the boundary layer were found to be higher than predicted by simple planing theory.

1. Introduction

Model scale experiments for use in CFD validation work were performed in the Clearwater Towing Tank at the National Research Council of Canada's Institute for Marine Dynamics and consisted of a series of resistance tests of a planing vessel. Tests were conducted over a range of speeds and in 6 different ballast configurations (displacement and longitudinal center of gravity). Measurements were made of tow force, running trim and sinkage, hull pressures, wetted surface area, and wave profiles. Additional tests were done to measure the boundary layer thickness at two locations along the hull using a laser Doppler velocimeter. These were performed for four speeds in a single ballast configuration. The boundary layer at each position and at each speed was delineated using about 20 runs. This paper describes the model and test setup, the test program, and examples of the measured data.

2. Model and tow arrangement

Planing boat model

The hull shape used in the experiments discussed in this paper was a 1:8 scale model of a full scale vessel currently in operation. It was constructed out of carbon fiber reinforced plastic strengthened with transverse and longitudinal stiffeners, a watertight bulkhead near the stern, and a shear deck with coaming. A plastic splash guard cover was fitted during tests.

The hull surface, shown in Figure 1, was marked with station numbers on the bottom and port side. Knife edges extending 1mm from the hull surface, were fitted along the chines to promote flow separation. The hull was not prismatic but did have a simple shape as shown in Figure 2. This cross section was constant from the transom for about 2/3 the length of the hull (covering the wetted length of the model for all ballast conditions when planing). A small flat bottom area at the centerline turns to a low deadrise of 5.9°. This deadrise then turns sharply to 40.8° near the chine (see Figure 2).

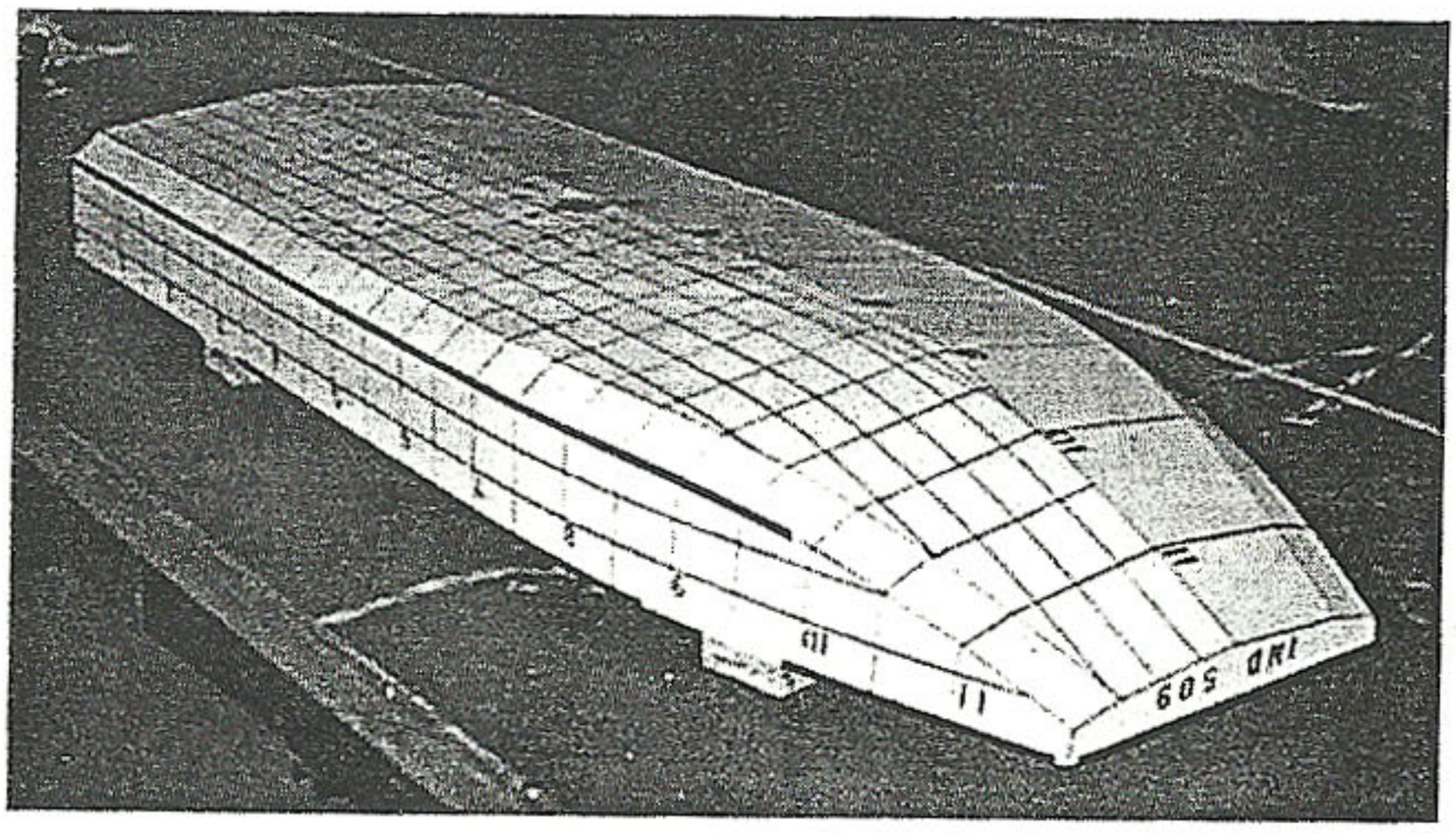

Figure 1. Model hull (LOA = 1.475m).

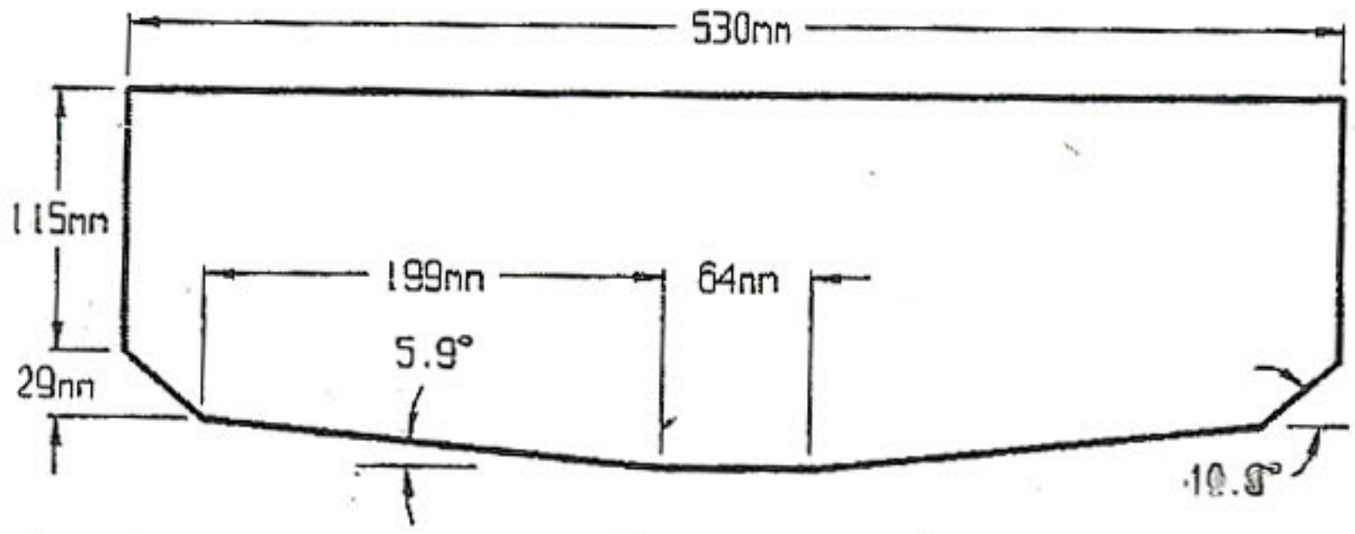

Figure 2. Model hull cross section.

Tow arrangement

The experiments were performed at NRC/IMD's Clearwater Towing Tank. The tank is 200 m long, 12 m wide, 7 m deep and contains fresh water. The 14 m long tow carriage has a maximum speed of 10.0 m/s. The model was fitted to the tow carriage using a gimbal and yaw restraint. Tow force was transmitted from the heave post through a linear bearing to an 'S'-shaped load cell (max. load = 50 lb.) and then through a universal joint to the model (see Figure 3). The universal joint allowed the model to pitch and roll freely and the heave post was free to move vertically in the tow post arrangement. The model was prohibited from rotating about the heave post by a yaw restraint which was counterbalanced so that it did not affect the ballast. The tow arrangement is shown in Figure 4.

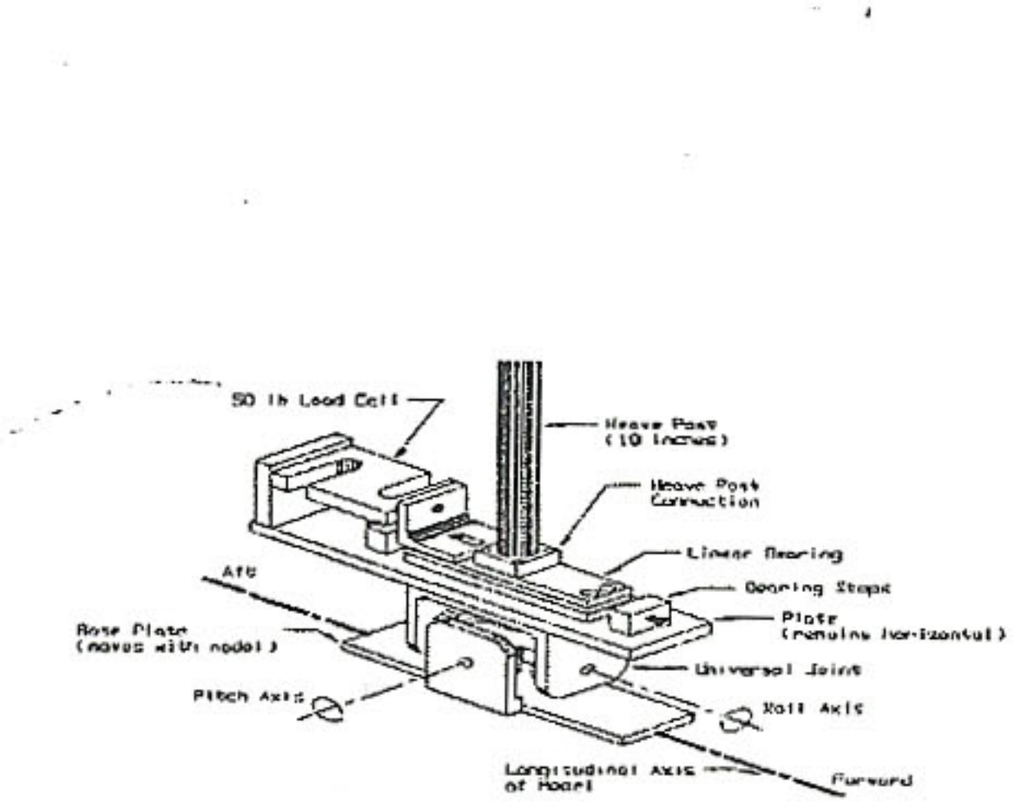

Figure 3. Gimbal.

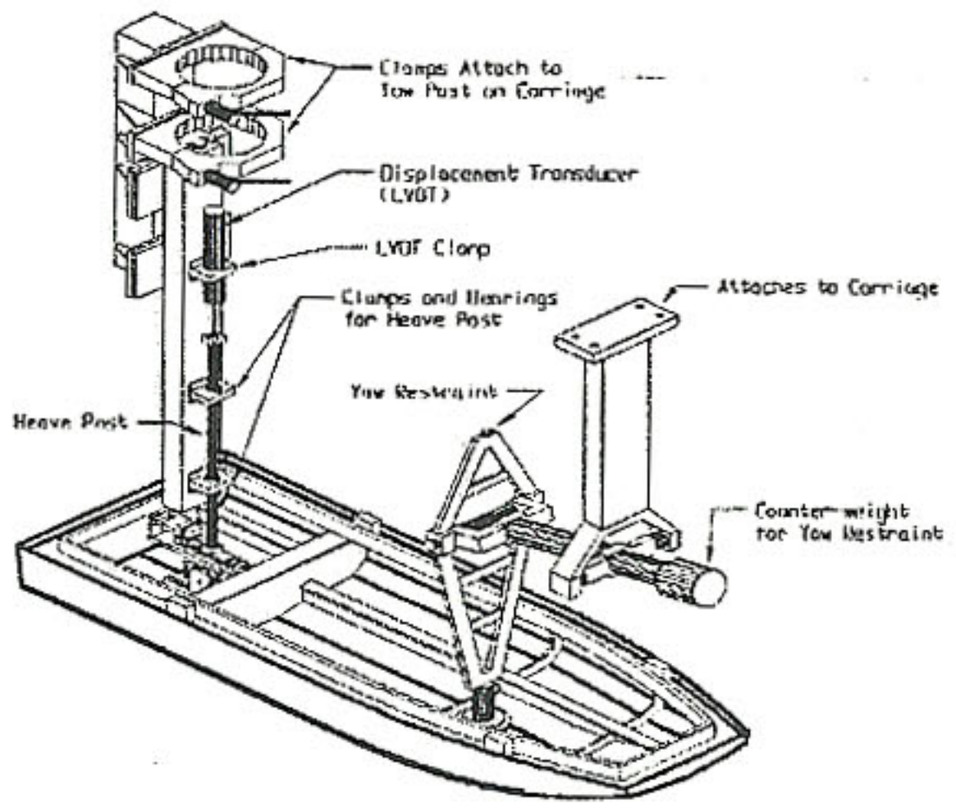

Figure 4. Tow arrangement.

3. Test program

The test program consisted of two phases. The first phase focused on testing the effects of different ballast conditions over a range of speeds. Measurements were made of tow force, running trim, sinkage, hull pressures, wetted surface areas, and wave profiles. The second phase was performed solely at the design ballast condition, and was used to measure boundary layer velocity profiles below the hull surface using a laser Doppler velocimeter (LDV).

As planing craft performance is sensitive to ballast condition, tests were performed over a range of displacements and locations of the longitudinal center of gravity (LCG). These conditions are given in Table 1, which also shows the static trim angles of the model. The first column lists the three displacements (design displacement

±15%) and the first row lists the three LCG positions (design LCG ±7%). LCG position was referenced from the transom base.
A plan view of the model hull bottom is given in Figure 5 showing the relative locations of the LDV windows, pressure transducers (labeled P1 through P9), tow point, and LCGs.

Table 1. Static trim angles for ballast conditions.

Displacement	LCG = 0.49 m	LCG = 0.53 m	LCG = 0.57 m
25.2 kg	-	1.0°	-
29.6 kg	2.0°	1.1°	0.4°
33.9 kg	-	1.3°	-

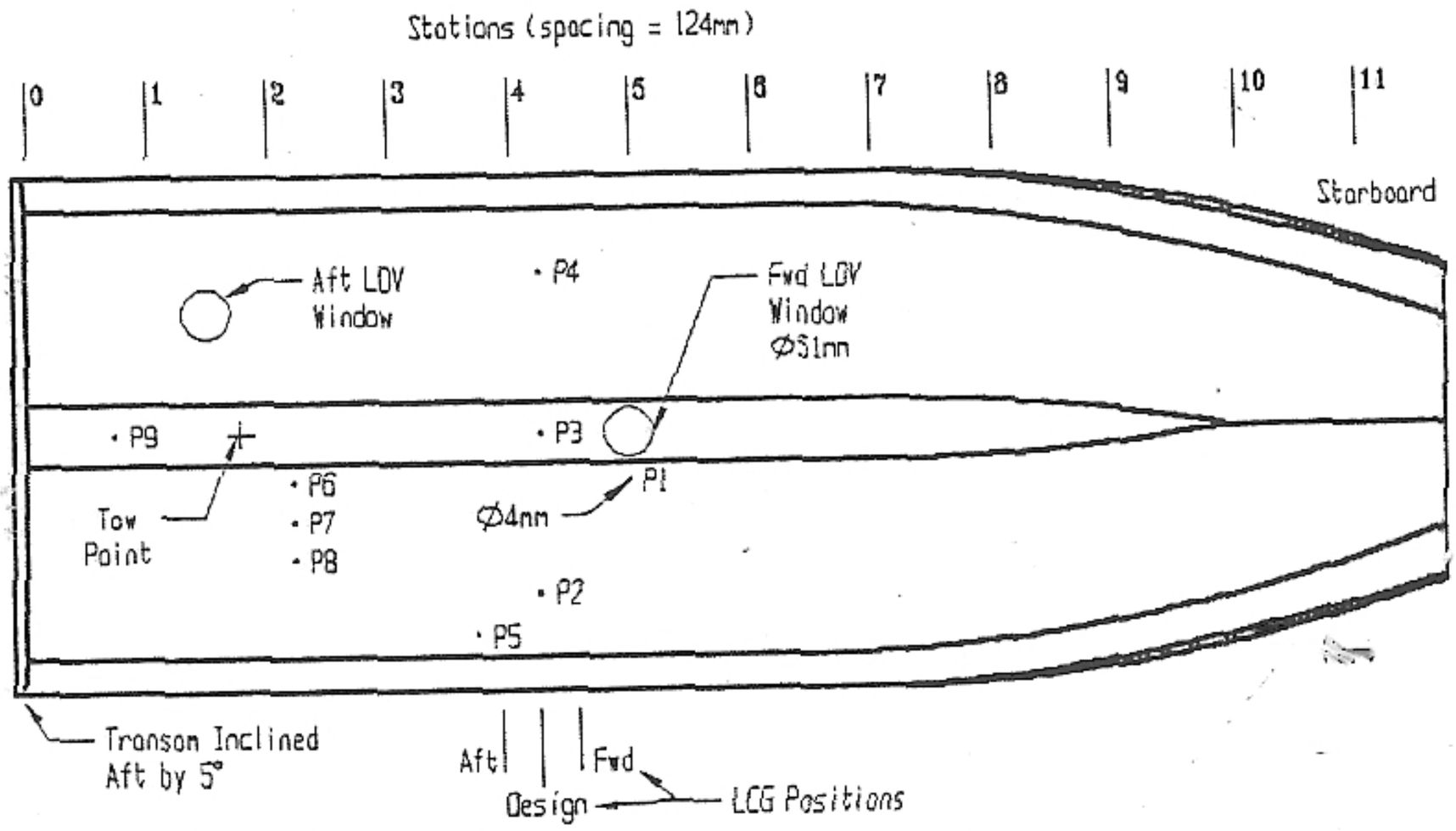

Figure 5. Instrument positions in model.

4. Results

Resistance

The resistance curves for the model were typical for a planing vessel and had the characteristic 'hump' speed at the onset of planing. Figure 6 shows the resistance results for the various ballast conditions. Only the design condition was tested over the full speed range. The curves closest to the design condition show the effect of a

7% change of LCG (both fore and aft) on resistance, while the two more distant curves show the effect of a 15% change in displacement.

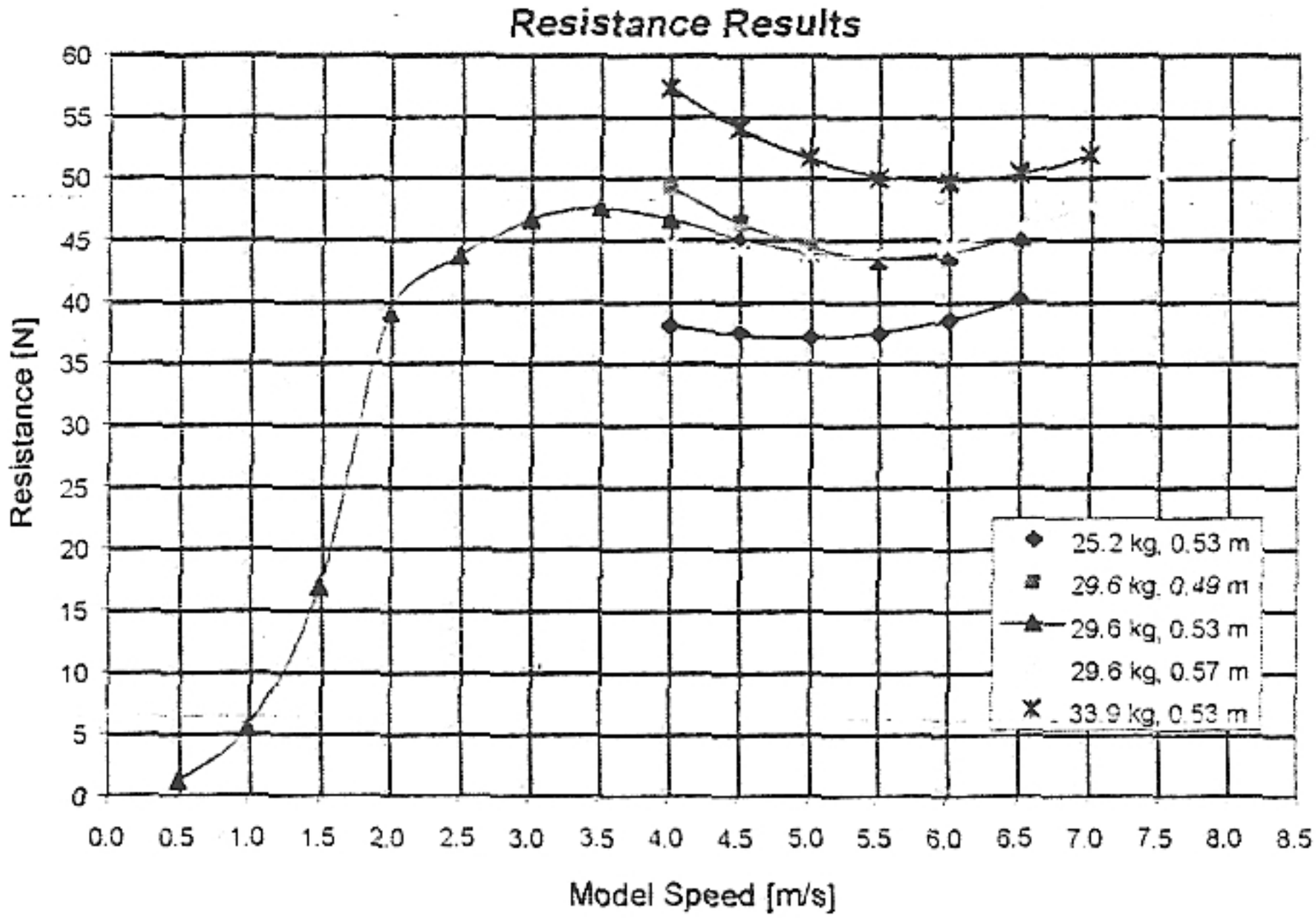

Figure 6. Model scale resistance.

Running Trim

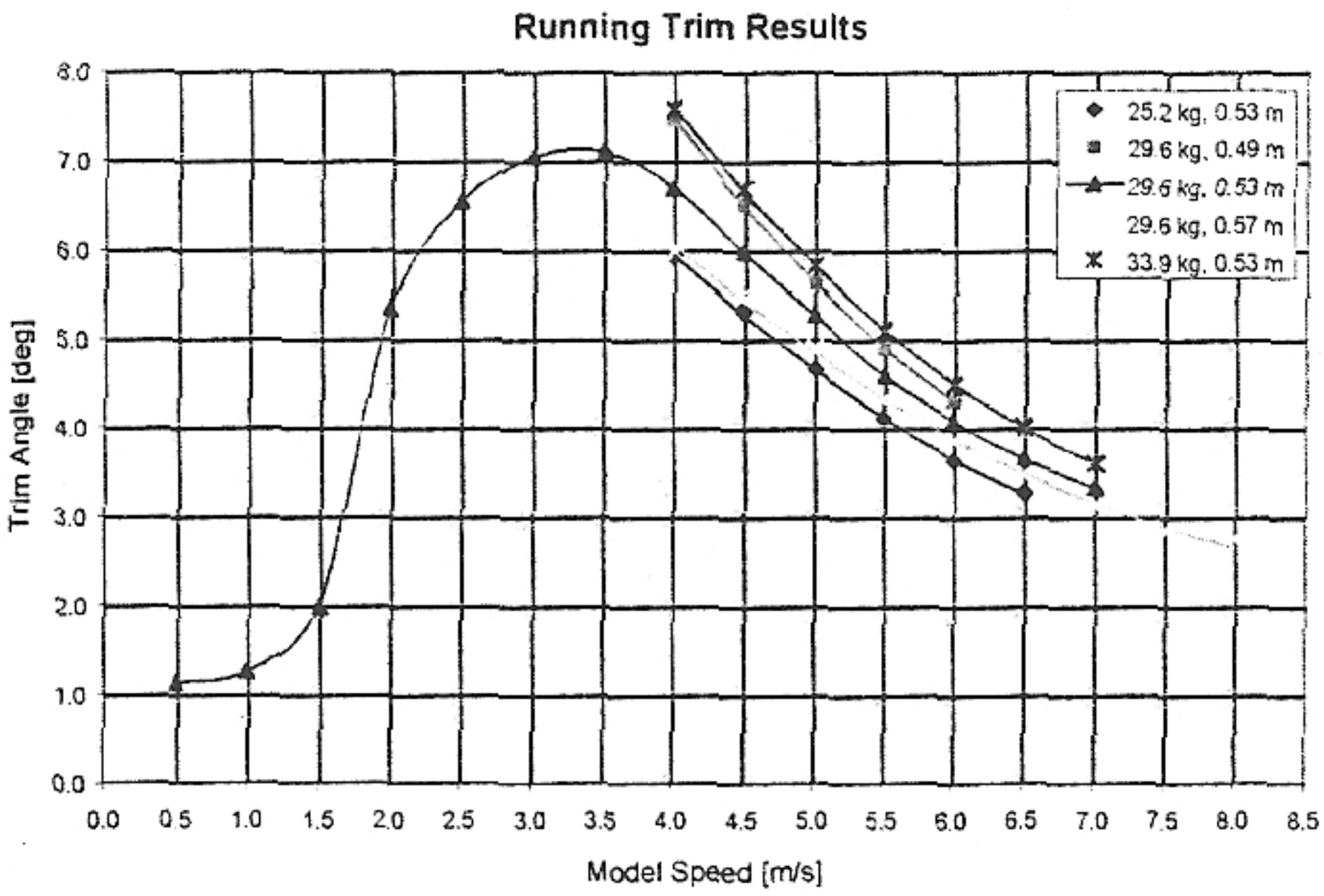

Figure 7. Running trim.

Trim angle is an important factor in planing craft performance as it changes the geometry of the hull relative to the water. The running trim angles for this model followed similar trends as the resistance curves, clearly identifying the 'hump' speed at which planing begins. Shown in Figure 7 are the absolute running trims for the various ballast conditions.

It can be seen from the plots that the different ballast conditions were not tested to the same maximum speeds. For instance, the aft LCG ballast condition was only tested to 6.0 m/s and the forward LCG condition was tested to 8.0 m/s. This occurred because the model was prone to dynamic instability, or porpoising, at high speeds. The aft LCG position made the model susceptible to this instability at speeds above 6.0 m/s and therefore it was not tested beyond that limit.

Another way of presenting the running trim results is to plot the change in trim angle developed at speed from the static trim angle at rest (given in Table 1). This plot, Figure 8, shows that when in the planing regime, the threshold above which porpoising occurred was when the change in trim angle dropped below approximately 2.1°. More details of the porpoising characteristics of this model can be found in Thornhill et al. (2000).

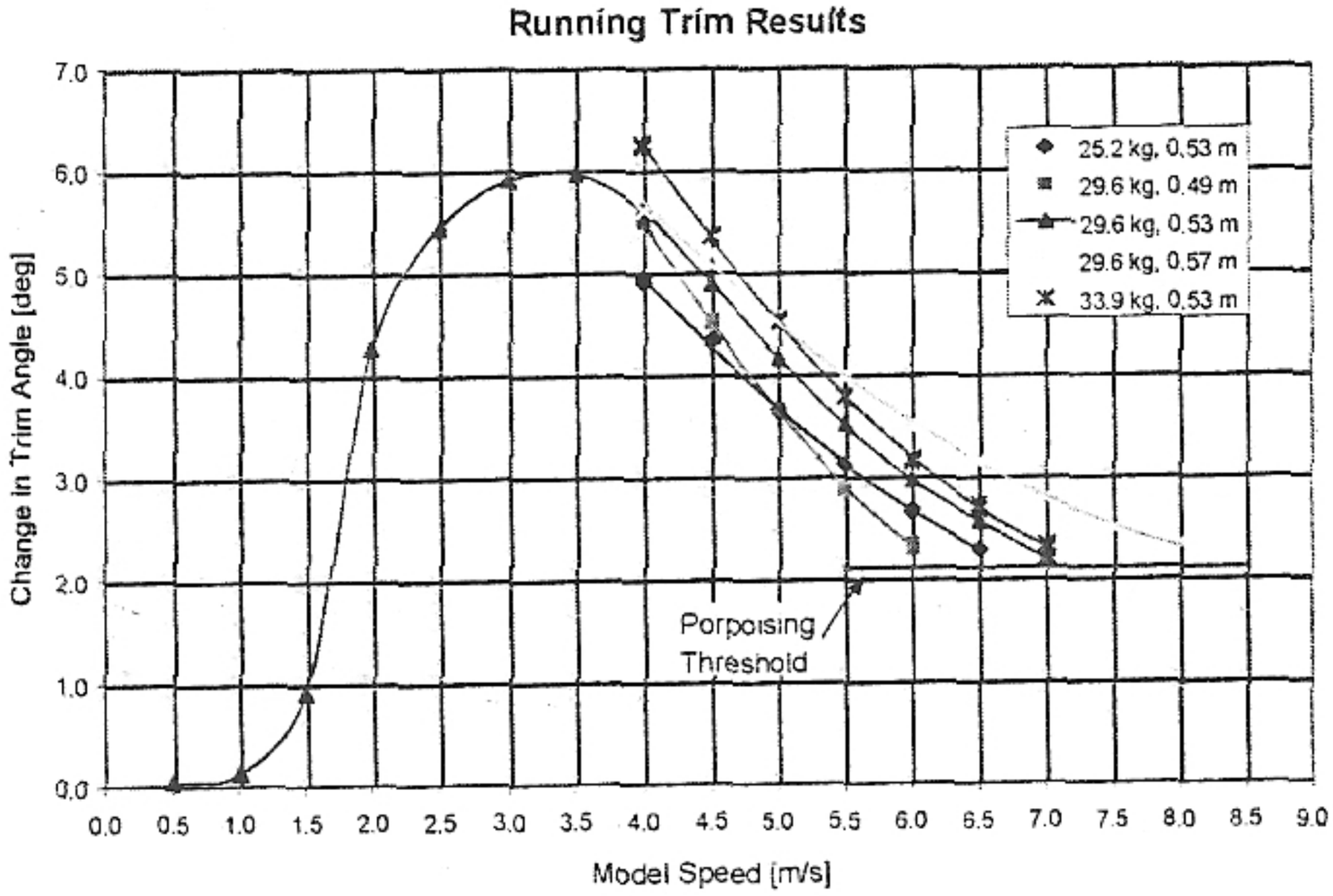

Figure 8. Change in trim.

Sinkage results

Sinkage refers to the change in the vertical position of the model at speed and was measured using an LVDT (linear voltage differential transducer) mounted on top of the heave post (see Figure 4). Shown below in Figure 9 is the sinkage profile for the design ballast condition. Also given in the figure is the trim profile for this condition.

These are presented together because sinkage is related to trim angle (the model did not necessarily rotate about the tow point where sinkage was measured). At low speeds, the model began to trim by the stern and sank downwards in the water. As it climbed its bow wave, trim peaked and then began to decrease while the model continued to rise upwards. At high speeds, trim angle continued to decrease while the vertical position leveled off to approximately 3.5cm above its original position.

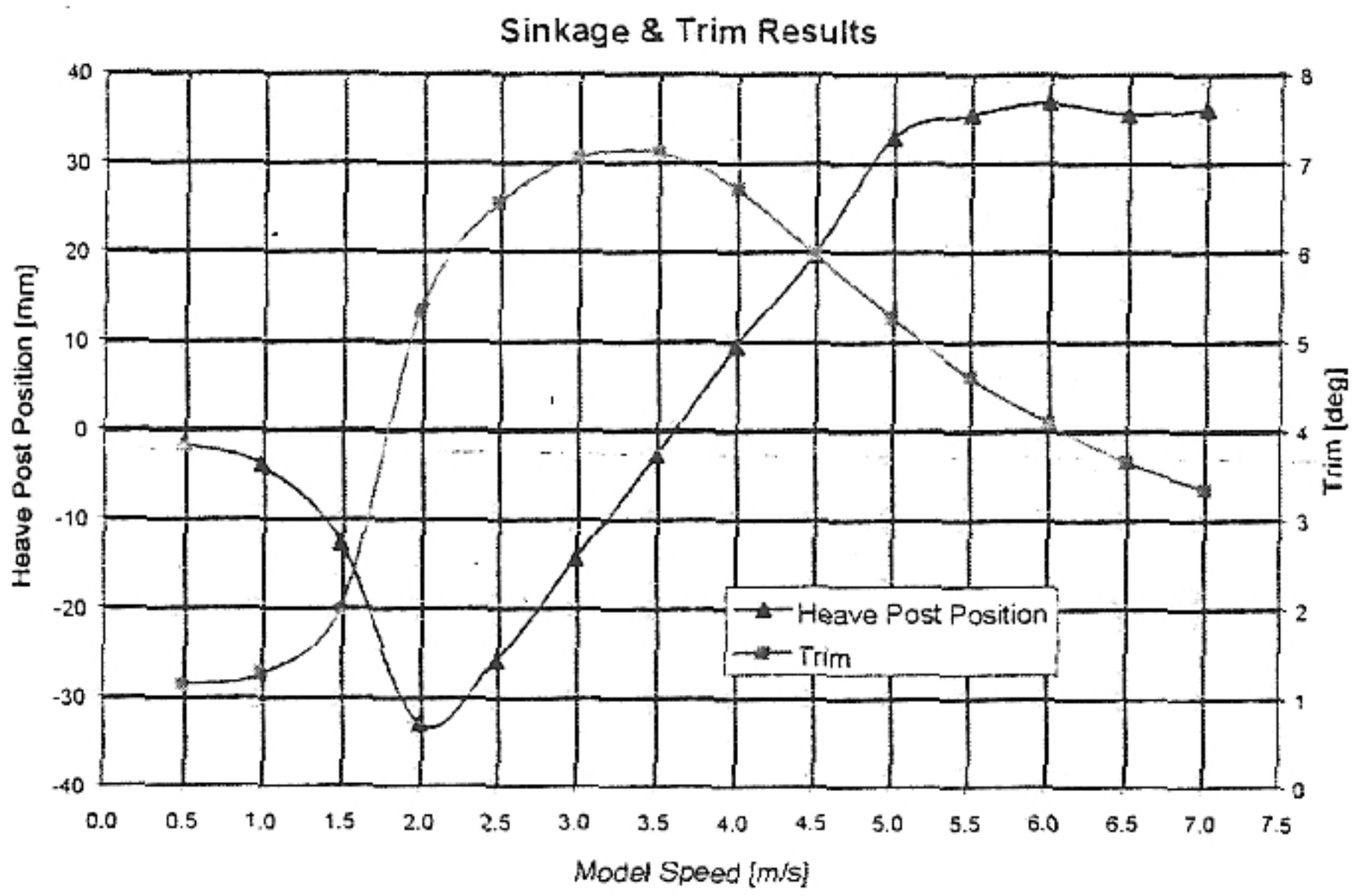

Figure 9. Sinkage and trim results.

Hull pressures

Hull pressures on the model were measured using 9 pressure taps mounted flush to the hull bottom at various locations. Several of these pressure taps malfunctioned during tests while others encountered relatively high levels of noise. The final results could not therefore be relied upon for specific quantitative information of the pressure distribution on the hull. They can, however, be used to show the range of pressure on the hull and identify certain trends that developed with increasing model speed. The most notable of these are shown in Figure 10.

The figure gives the results from two pressure transducers located fore and aft at the same longitudinal plane in the model (P1 and P6 shown in Figure 5). The forward transducer records increasing pressure with increasing speed, while the aft transducer shows the opposite trend, with negative pressure values at high speeds. These negative pressure values correspond to increased flow velocities near the hull as discussed in a later section.

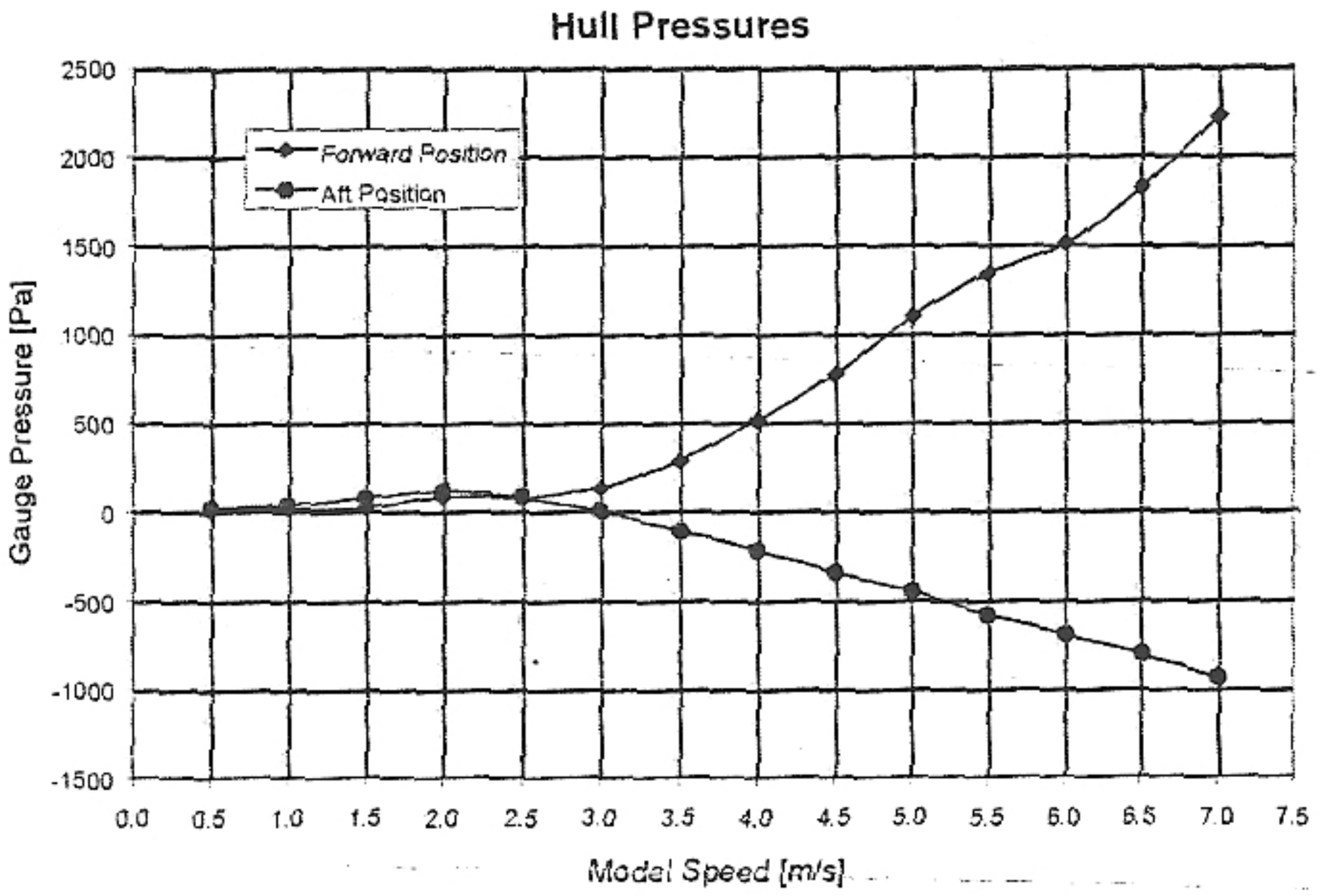

Figure 10. Hull pressure at two locations.

Wave profiles

The surface wave profiles produced by the model at speed were captured by a transverse array of capacitance probes located midway along the tow tank. The 23 probes were spaced 7 inches apart, the first being 7 inches from the side of the model as it passed by. Sampled at 100 hz, the time traces from the probes show the wave elevations at the various longitudinal cuts. A proximity switch was used to correlate the position of the model with the probe data: when the switch was triggered, the model's bow was in line with the probe array. The probe array is shown in Figure 11 attached to a beam fixed to the tank wall. An example of the data collected from the probes is shown in Figure 12.

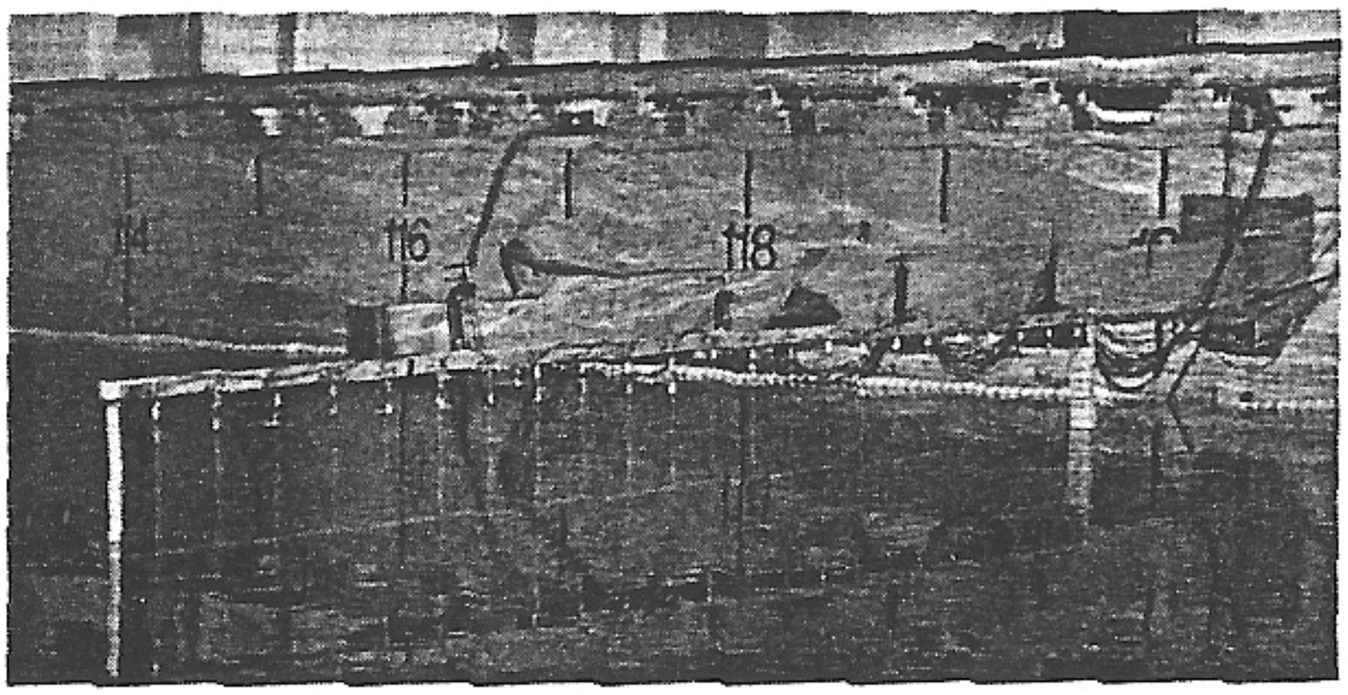

Figure 11. Wave probe array in tank.

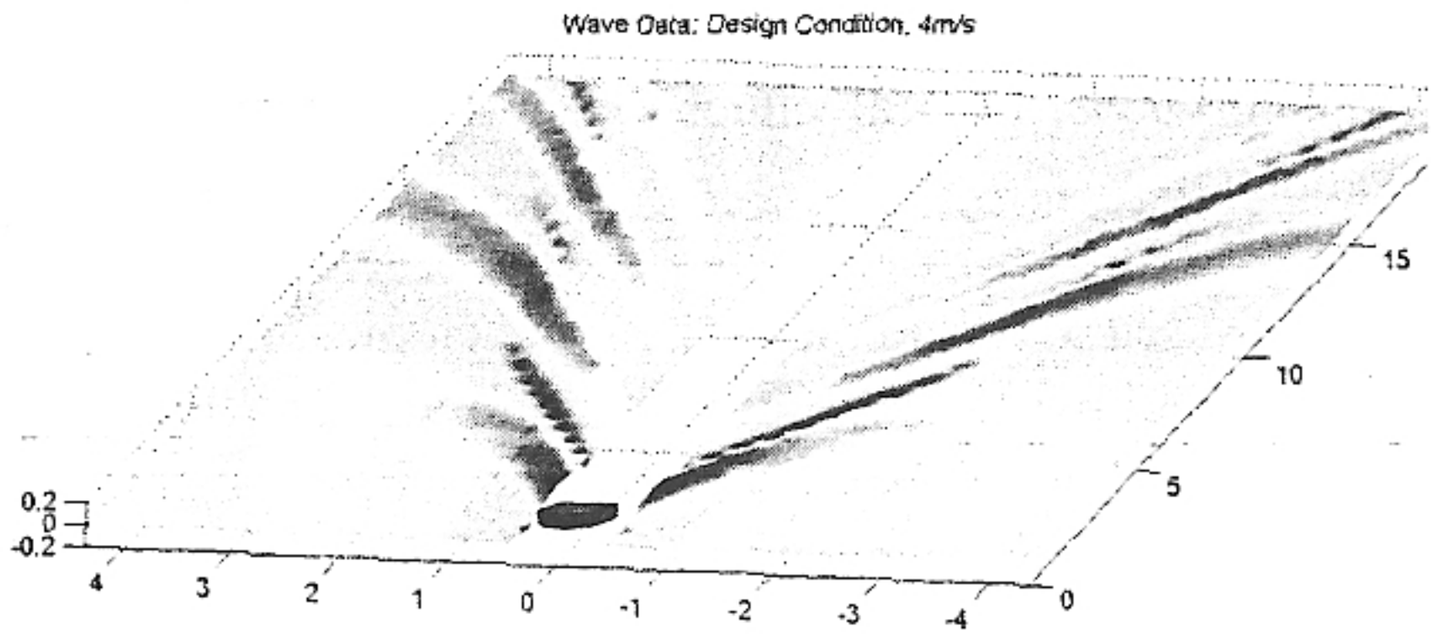

Figure 12. Wave probe data.

Boundary layer velocity profiles

The second phase of the experimental program was dedicated to determining velocity profiles in the boundary layer at two locations for four different model speeds in the design ballast condition. The measurements were made using a laser Doppler velocimeter (LDV) fitted in the model. This instrument has several advantages over other more common techniques for velocity measurements such as pitot tubes and hot-film anemometry. The primary advantage of the LDV is its non-intrusiveness; only the laser beams enter the water, so they do not influence the thin layer of fluid where measurements are being taken.

The LDV uses intersecting laser beams to make velocity measurements. Strictly speaking, the LDV measures the velocity of particles in the flow and not the flow itself. A particle, when traveling through the volume of intersection of the beams, reflects light as it passes through an interference pattern of light and dark bands caused by the lasers of matching wavelength. Processors in the LDV determine the frequency of this pulsating reflected light picked up by sensors in the probe. As the distance between the interference bands is known, the processor can then calculate the velocity of the particle. Numerous particle measurements are averaged to determine the mean flow velocity. Particles are added as "seed" to the flow and are generally in the size range of 0.5 – 5.0 microns. The measurement volume of the LDV depends on both the beam diameter and the angle of intersection. For these experiments the volume was an ellipsoid 0.64 mm in height (perpendicular to the hull) and 76 μm in diameter.

Seeding is an important part of LDV testing as it controls both the data rate (the number of particles passing through the intersection volume per second) and validation (the percentage of particles that could be processed into velocity measurements). For these experiments, seed was added for each test by aiming a small stream of a concentrated water/seed mix in the path of the model. Several types of seed were used, including silver-coated glass micro-balloons and pre-sifted all-

purpose flour. Data rates for the experiments ranged from 30 Hz to 3 kHz with validation between 60-95%. Typical values for most tests were data rates around 500 Hz with 75% validation.

The set-up for the experiments had the LDV probe mounted inside the model on a set of micrometer tables used to locate the probe for each measurement. The probe faced downward and projected the lasers through a small acrylic window in the hull. The beams intersected at a point just below the window where a measurement was taken (see Figure 13). The micrometer tables were used to precisely position the probe at different positions within the boundary layer. A single run of the carriage was used to measure the velocity of each point in the boundary layer at each model speed. Successive runs were needed to resolve the velocity profile for a given model speed.

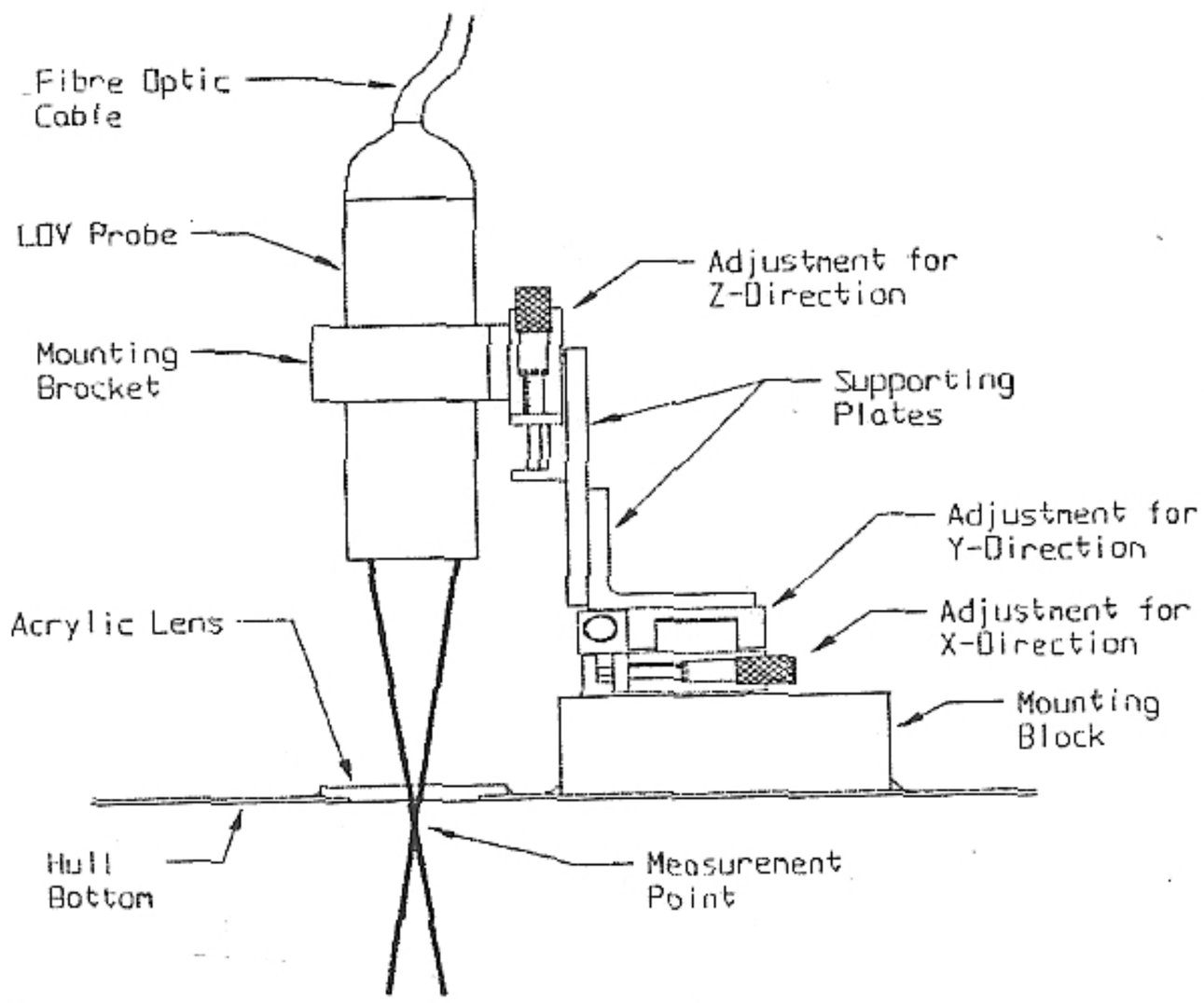

Figure 13. LDV mount.

Raw data from a typical test is given in Figure 14. It shows the acceleration, constant speed, and deceleration portions of the run. The figure also shows that the raw velocity data fell onto equally spaced discrete values (seen as bands of points). This feature is an artifact of the LDV's internal processors that determine the particle velocities. The width between these bands can be changed, but doing so also alters the range of velocities which can be measured. A smaller bandwidth results in a smaller velocity range. These experiments used a bandwidth of approximately 0.1 m/s.

Boundary layer velocity profiles for two positions on the hull for each of four model speeds (4 m/s, 5 m/s, 6 m/s and 6.5 m/s) were measured. Results for the model speed of 4 m/s are given below in Figure 15.

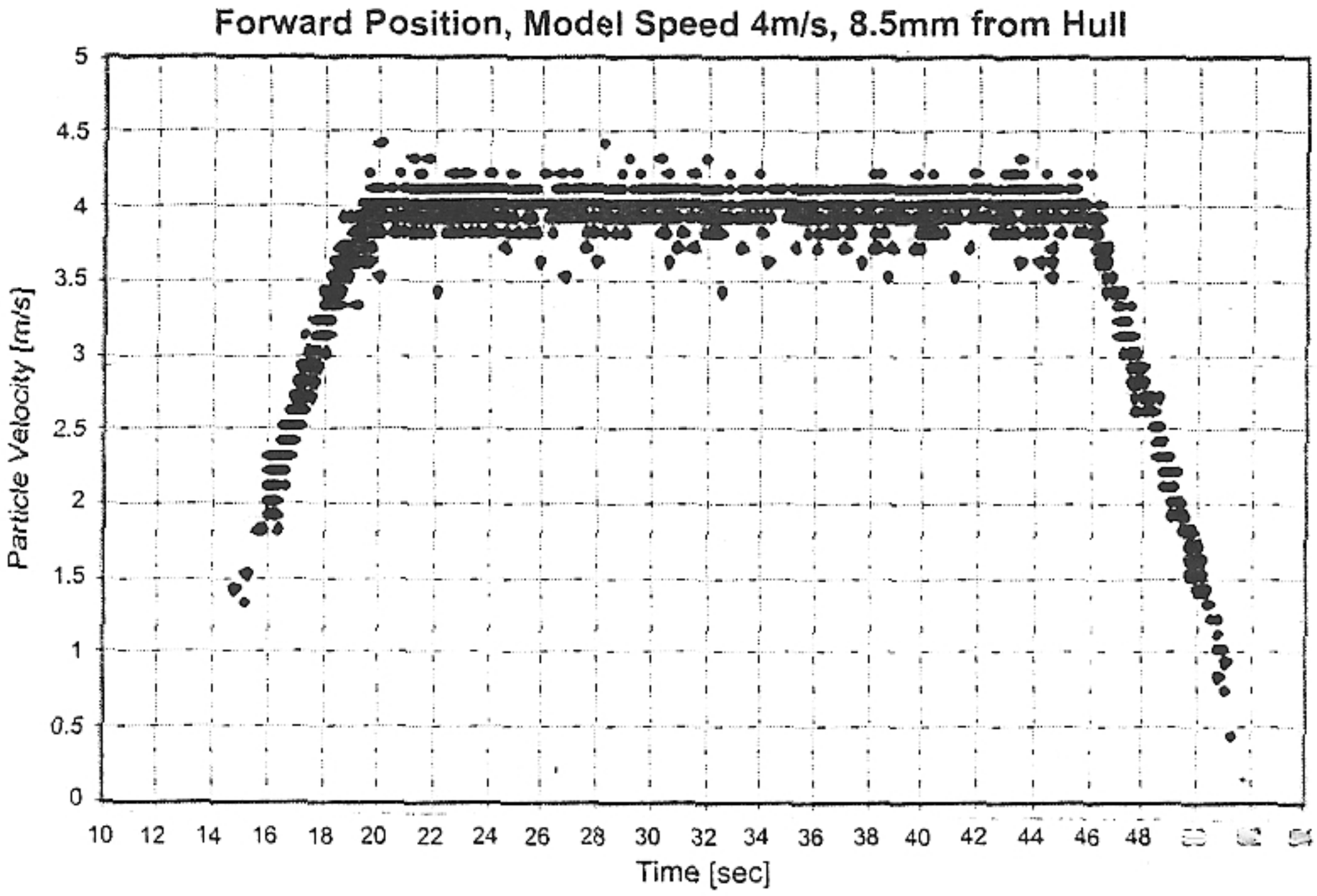

Figure 14. Typical LDV data.

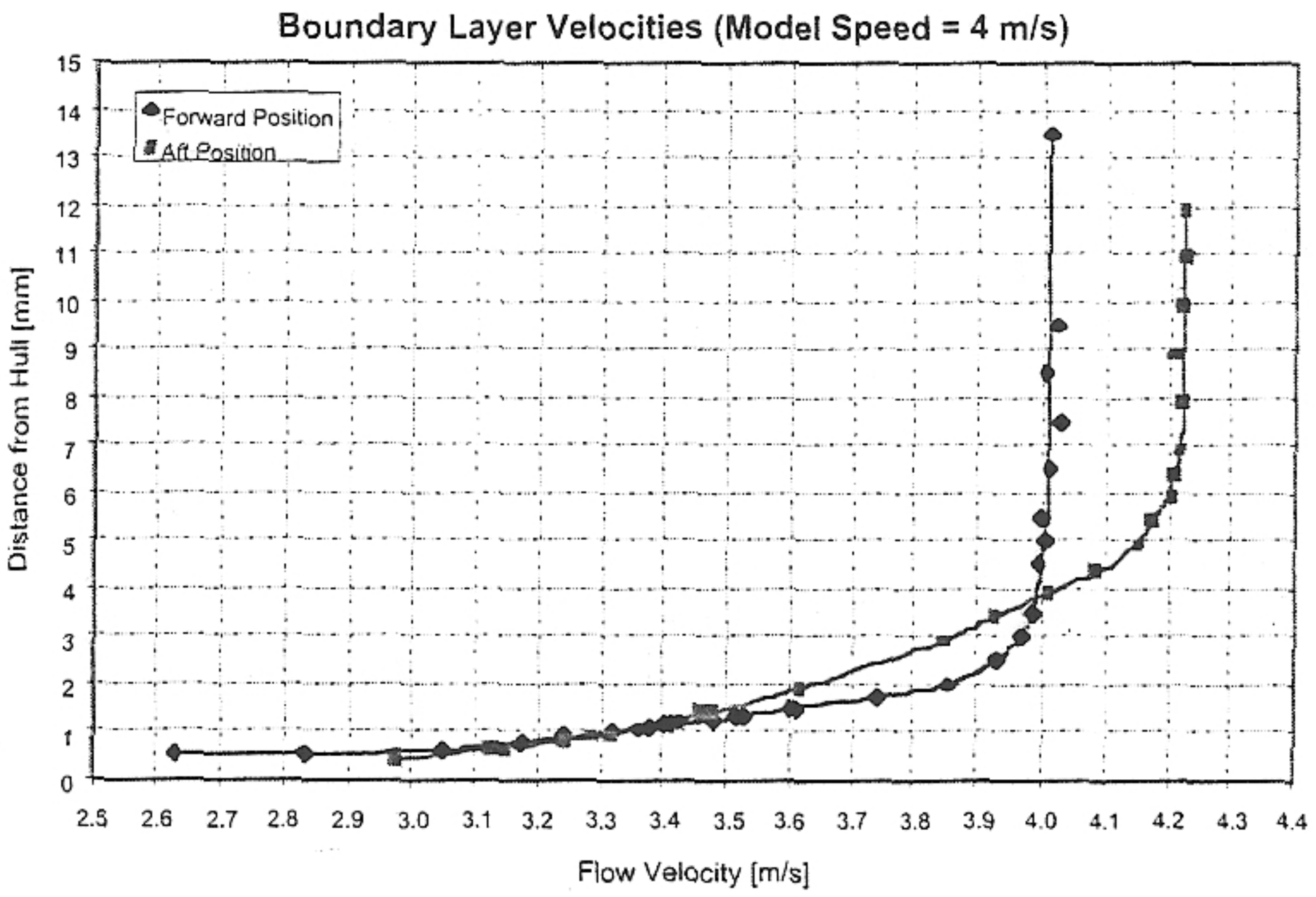

Figure 15. Boundary layer velocities (V_m = 4 m/s).

The results from these measurements clearly show the boundary layer velocity form, thickness, and the free stream velocity for both of the two locations at each speed tested (for a total of 8 profiles). In the figure, the forward position shows a boundary

layer thickness of about 4 mm with a free stream velocity equal to the model velocity. The aft position shows that the boundary layer had grown thicker and that the flow achieved a greater free stream velocity, exceeding that of the model speed. This is consistent with the negative pressures measured in the aft region of the hull. Profiles at the other model speeds tested were qualitatively similar as those shown in Figure 16. The percentage increase in free stream velocity from the forward to the aft position decreased as the model speed increased (trim angle also decreased). The boundary layer thickness also decreased with increasing model speed.

The positions of the forward and aft measurement positions relative to the leading edge of the wetted hull area for a given model speed are shown below in Figure 16.

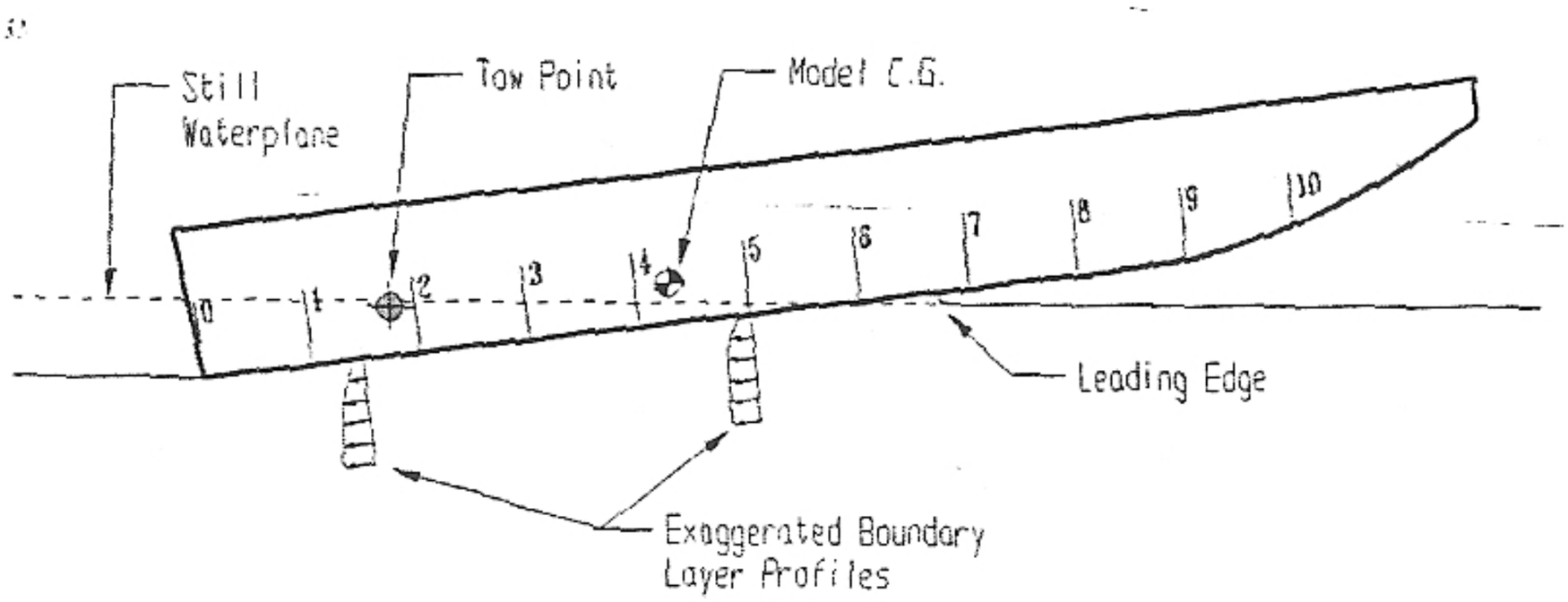

Figure 16. Vessel attitude (4 m/s).

One difficulty with the technique used to determine the boundary layer velocity profile was the determination of the reference or zero position of the hull surface. The procedure for finding this zero position consisted of systematically moving the measurement point closer to the lens until the photo-detectors gave an overload error. This meant that the measurement volume was inside the lens, and that the beams were reflecting directly back to the detectors. It was, however, possible that measurements could be taken with a small portion of the measurement volume inside of the lens, without overloading the photo-detectors. The size of this overlap could not be determined. The orientation of the probe meant that the largest dimension of the measurement volume (0.64mm) was perpendicular to the hull. It was assumed that measurements could not be made if more than half of the measurement volume was inside the lens. This gives an uncertainty in the hull zero position for the LDV measurements of approximately 0.32mm. The shape of the profiles is not affected by this bias, which would shift the entire curve up or down.

Another result from the analysis of the raw LDV data came from the standard deviations of the samples used to calculate the mean flow velocities. Shown Figure 17, the standard deviations followed a similar trend as the velocities. High standard deviations were measured close to the hull, while in the free stream they leveled off. The higher values close to the hull can be attributed to two primary factors:

turbulence and velocity gradient. Wall bounded turbulence in the boundary layer can cause fluctuations in velocity that would result in increased standard deviation. The large velocity gradient close to the hull would also result in increased standard deviation since a broader range of velocities spanning from the bottom to the top of the measurement volume would have been captured.

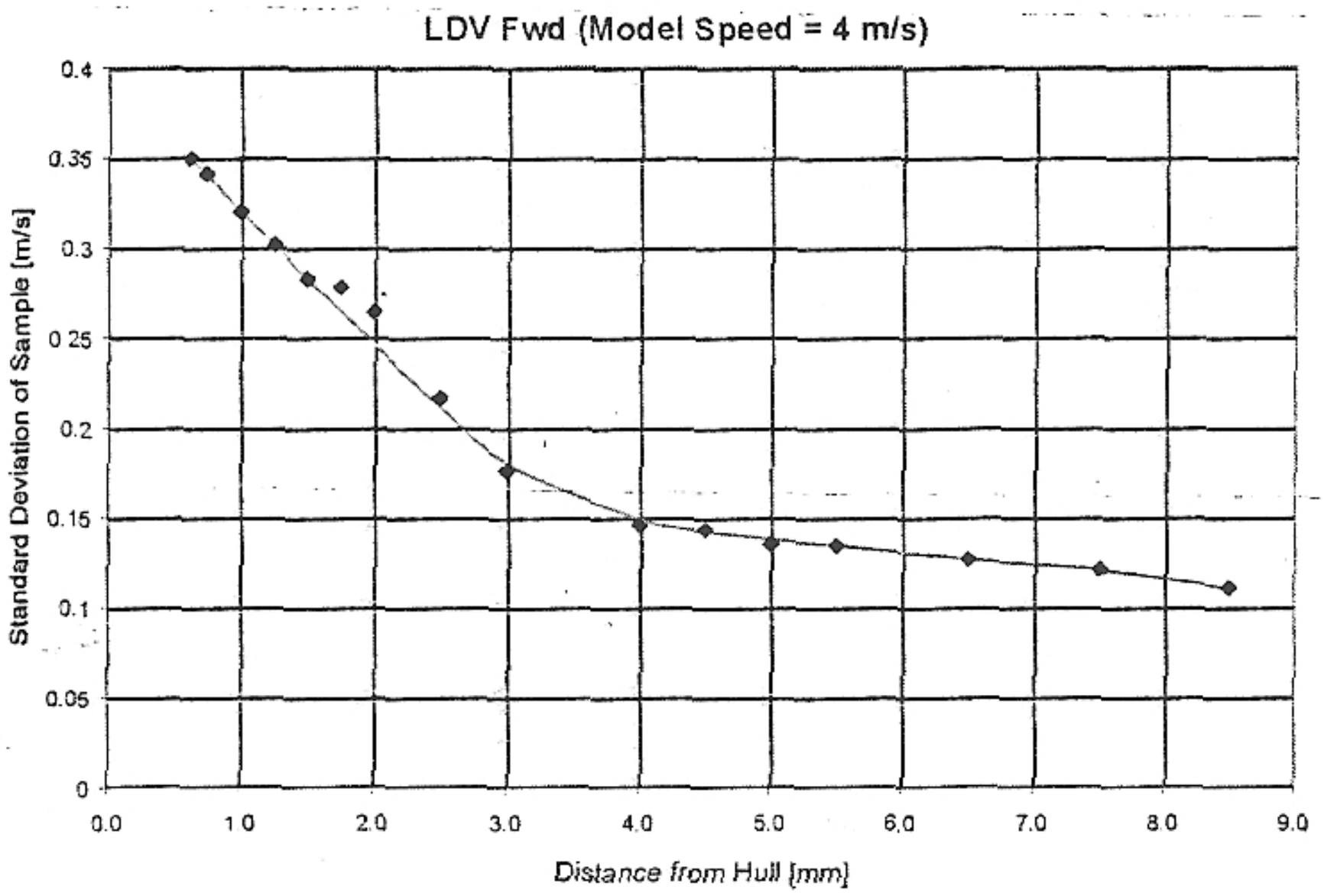

Figure 17. Standard Deviations from LDV Data.

Summary

Tests were performed on a 1/8 scale model of a planing vessel to generate a set of performance data to be used in future validation of numerical simulations. Sample results (full results can be found in Thornhill, 2002) were presented for the measurements of resistance, running trim, sinkage, hull pressures, wave profiles, and boundary layer velocity profiles. Resistance and running trim results showed characteristics common to planing craft. Hull pressures were found to increase in the forward part of the hull but decrease and become negative in the aft. Boundary layer thicknesses were found to increase in the direction of flow and to decrease with increasing model speeds as expected. Velocities measured just outside the boundary layer were found to be greater than free stream in the aft part of the hull, showing an acceleration from the forward position.

Acknowledgements

These experiments were performed at the National Research Council of Canada's Institute for Marine Dynamics (NRC/IMD). In addition to NRC/IMD, funding and technical assistance was also provided by Memorial University of Newfoundland, Oceanic Consulting Corporation, and NSERC (Natural Sciences and Engineering Research Council).

NRC/ Institute for Marine Dynamics	http://www.nrc.ca/imd/
Memorial University of Newfoundland	http://www.engr.mun.ca/
Ocean Engineering Research Centre	http://www.engr.mun.ca/OERC/
Oceanic Consulting Corporation	http://www.oceaniccorp.com/
NSERC	http://www.nserc.ca/

References

[1] Thornhill E., Application of a General CFD Code to Planing Craft Performance, Ph.D. Thesis submitted to the Memorial University, Faculty of Engineering and Applied Science, St. John's Newfoundland, Canada, 2002.

[2] Thornhill E., Veitch B., Bose N., Dynamic Instability of a High Speed Planing Boat Model. *Marine Technology*, July 2000.

[3] Savitsky D., Hydrodynamic Design of Planing Hulls, *Marine Technology*, vol. 1, no. 1, pp. 71 – 95, October 1964.

[4] Du Cane P., *High Speed Small Craft 3rd Ed.* Temple Press Books, London. 1964.

[5] Payne P.R., *Design of High Speed Boats Volume 1: Planing*. Fishergate Inc. Annapolis. 1988.